

Numerical Analysis of Specific Absorption Rate and Heat Transfer in the Human Body Exposed to Leakage Electromagnetic Field at 915 MHz and 2450 MHz

Teerapot Wessapan
Siramate Srisawatdhisukul
Phadungsak Rattanadecho
e-mail: ratphadu@engr.tu.ac.th

Department of Mechanical Engineering,
Research Center of Microwave Utilization in
Engineering (RCME),
Faculty of Engineering,
Thammasat University (Rangsit Campus),
Pathumthani 12120, Thailand

In recent years, society has increased utilization of electromagnetic radiation in various applications. This radiation interacts with the human body and may lead to detrimental effects on human health. However, the resulting thermophysiological response of the human body is not well understood. In order to gain insight into the phenomena occurring within the human body with temperature distribution induced by electromagnetic field, a detailed knowledge of absorbed power distribution is necessary. In this study, the effects of operating frequency and leakage power density on distributions of specific absorption rate and temperature profile within the human body are systematically investigated. This study focuses attention on organs in the human trunk. The specific absorption rate and the temperature distribution in various tissues, obtained by numerical solution of electromagnetic wave propagation coupled with unsteady bioheat transfer problem, are presented. [DOI: 10.1115/1.4003115]

Keywords: microwave, temperature distribution, specific absorption rate, human body

1 Introduction

Electromagnetic (EM) energy is a one heat source that is attractive over conventional heating methods because an electromagnetic wave that penetrates the surface is converted into thermal energy within the material volumetrically. High speed startup, selective energy absorption, instantaneous electric control, nonpollution, high energy efficiency, and high product quality are several advantages of microwave heating. Therefore, this technology is used in many industrial and household applications such as heating process [1] and drying process [2]. Rapid development of electromagnetic energy applications causes an increase in public concern about health risks from electromagnetic energy emitted from various sources [3].

Increasing use of high power electromagnetic energy results in the necessity to identify the limits of safe exposure with respect to thermal hazards. The amount of energy absorbed by tissue depends on many factors including frequency, dielectric property of the tissue, irradiating time exposure, intensity of electromagnetic radiation, and water content of the tissue. For this reason, public organizations throughout the world have established safety guidelines for electromagnetic wave absorption values [3]. For human exposure to electromagnetic fields, these guidelines are based on peak spatial-average specific absorption rate (SAR) for human body tissues.

The power absorption in human tissues induces temperature increase inside tissues. The severity of the physiological effect produced by small temperature increases can be expected to worsen in sensitive organs. An increase in approximate 1–5°C in

human body temperature can cause numerous malformations, temporary infertility in males, brain lesions, and blood chemistry changes. Even a small temperature increase in human body (approximately 1°C) can lead to altered production of hormones and suppressed immune response [4].

In the past, the experimental data on the correlation of SAR levels to the temperature increases in human body are sparse. There is a research on SAR distribution of three-layer human body, which simulates three-layer physical models of skin, fat, and muscle tissues [5]. There are limited data available on thermal properties and dielectric properties of human tissues, as very few epidemiological studies have been conducted. There are some experimental studies in animals such as rat [6], cow [7], and pig [8]. However, the results may not represent the practical behavior of human tissues. Most previous studies of human body exposed to electromagnetic field did not consider heat transfer, resulting in an incomplete analysis. Therefore, modeling of heat transport in human tissues is needed in order to completely explain. The modeling of heat transfer in human tissues has been investigated. Earlier studies of heat transfer in human tissues utilized the general bioheat equation [9]; thereafter, the coupled model of general bioheat equation and Maxwell's equation were used to model human tissues exposed to electromagnetic field [10]. Other researches have been done for temperature distribution over the surface, and the various biotissues exposed to an electric field have been studied [11,12]. Furthermore, few reports have suggested thermal interactions for microwave frequency fields [13]. Researchers also carried out temperature increases in human head exposed to a handheld cellular phone [14–17].

However, most studies of temperature increases induced by electromagnetic waves have not been considered in a realistic domain of the human body with complicated organs of several types of tissues. There are few studies on the temperature and electromagnetic field interaction in realistic physical model of the human

Contributed by the Heat Transfer Division of ASME for publication in the JOURNAL OF HEAT TRANSFER. Manuscript received January 6, 2010; final manuscript received November 17, 2010; published online xxx-xxxx-xxxx. Assoc. Editor: Darrell W. Pepper.

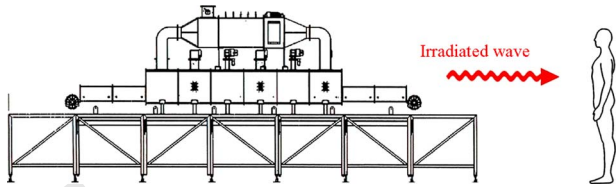


Fig. 1 Wave leakage from an electromagnetic radiation device

body due to the complexity of the problem, even though it is directly related to the thermal injury of tissues. Therefore, in order to provide information on levels of exposure and health effects from electromagnetic radiation adequately, it is essential to simulate the coupled electromagnetic field and heat transfer within an anatomically based human body model to represent the actual process of heat transfer within the human body.

This research is a pioneer work that simulates the SAR distribution and temperature distribution over an anatomically based human body. In this research, a two-dimensional human cross section model [18] was used to simulate the SAR distribution and temperature distribution over the human body at different frequencies. Electromagnetic wave propagation in tissues was investigated by using Maxwell's equations. An analysis of heat transfer in human tissues exposed to microwaves was investigated by using the bioheat equation. The effects of operating frequency (915 MHz and 2450 MHz) and leakage power density (5 mW/cm², 10 mW/cm², 50 mW/cm², and 100 mW/cm²) on distributions of specific absorption rate and temperature profile within the human body are systematically investigated. The 915 MHz and 2450 MHz frequencies were chosen for simulations in this study as they have wavelengths in the microwave band and are used most frequently in the application of industrial high power microwave

heating. The obtained values provide an indication of limitations that must be considered for temperature increases due to localized electromagnetic energy absorption.

2 Formulation of the Problem

Electromagnetic fields emitted by high power radiation devices are harmful. Figure 1 shows the leakage of electromagnetic energy from the industrial microwave drying system to a human body. It is known that a human body exposed to intense electromagnetic waves can cause significant thermal damage in sensitive tissues within the human trunk. Therefore, it is necessary to investigate the temperature distributions due to exposure to electromagnetic waves in order to investigate the hot spot zones within the human body especially in abdominal and thoracic cavities.

Due to ethical consideration, exposing a live human body to electromagnetic fields for experimental purposes is difficult. It is more convenient to develop a realistic model through numerical simulation. The next section, an analysis of specific absorption rate and heat transfer in the human body exposed to electromagnetic field is illustrated. The system of governing equations as well as initial and boundary conditions are solved numerically using the finite element method (FEM).

3 Methods and Model

The first step in evaluating the effects of a certain exposure to radiation in the human body is the determination of the induced internal electromagnetic field and its spatial distribution. Thereafter, electromagnetic energy absorption, which results in temperature increases within particular parts of the human body and other interactions, can be considered.

3.1 Human Model. From Fig. 2, a two-dimensional human body model used in this study is obtained by the image processing technique from the work of Shiba and Higaki [18]. The model has

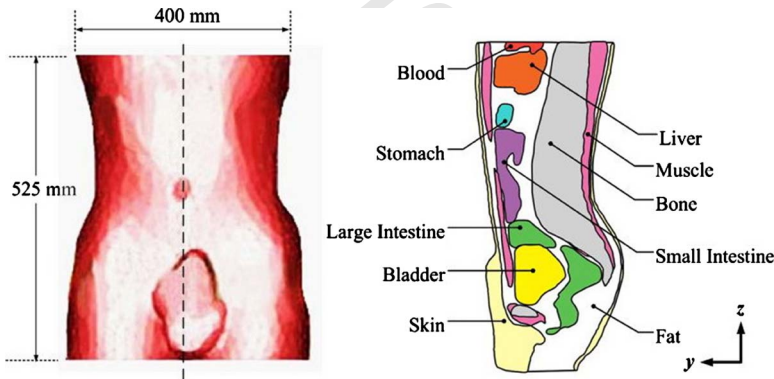


Fig. 2 Human body vertical cross section [16]

Table 1 Dielectric properties of tissues

Tissue	ρ (kg/m ³)	σ (S/m)	915 MHz		2450 MHz	
			ϵ_r	σ (S/m)	ϵ_r	σ (S/m)
Skin	1125	0.92	44.86	2.16	41.79	
Fat	916	0.09	5.97	0.13	5.51	
Muscle	1047	1.33	50.44	1.60	46.40	
Bone	1038	2.10	44.80	2.10	44.80	
Large intestine	1043	2.04	53.90	2.04	53.90	
Small intestine	1043	3.17	54.40	3.17	54.40	
Bladder	1030	0.69	18.00	0.69	18.00	
Blood	1058	2.54	58.30	2.54	58.30	
Stomach	1050	2.21	62.20	2.21	62.20	
Liver	1030	1.69	43.00	1.69	43.00	

Table 2 Thermal properties of tissues

Tissue	k (W/m K)	C_p (J/kg K)	ω_b	Q_{met} (W/m ³)
Skin	0.35	3437	0.02	1620
Fat	0.22	2300	4.58×10^{-04}	300
Muscle	0.6	3500	8.69×10^{-03}	480
Bone	0.436	1300	4.36×10^{-04}	610
Large intestine	0.6	3500	1.39×10^{-02}	9500
Small intestine	0.6	3500	1.74×10^{-02}	9500
Bladder	0.561	3900	0.00×10^{00}	
Blood	0.45	3960		
Stomach	0.527	3500	7.00×10^{-03}	
Liver	0.497	3600	0.017201	

a dimension of 400 mm in width and 525 mm in height. This model comprises ten types of tissues, which are skin, bone, muscle, fat, nerve, blood, and so forth. These tissues have different dielectric and thermal properties. The thermal properties and dielectric properties of tissues at the frequencies of 915 MHz and 2450 MHz are given in Tables 1 and 2, respectively. As very few studies associated with human tissue properties have been conducted, some of the tissue properties are not quantified. It is also difficult to directly measure tissue properties of a live human. Therefore, we used an assumption of comparing them to animal tissues (it should be noted that the properties based on animal experiments are used for most thermal parameters because no actual data are available for the parameters of the human model). Figure 2 shows a vertical cross section through the middle plane of the human trunk model.

3.2 Equations for Electromagnetic Wave Propagation Analysis. Mathematical models were developed to predict the electric field, SAR, and temperature distribution within the human body. To simplify the problem, the following assumptions were made.

1. Electromagnetic wave propagation is modeled in two dimensions over the y-z plane.
2. The human body in which electromagnetic waves and human body interact proceeds in the open region.
3. The computational space is truncated by scattering boundary condition.
4. In the human body, an electromagnetic wave is characterized by transverse electric fields (TE mode).

5. The model assumes that dielectric properties of tissues are constant.

The electromagnetic wave propagation in the human body is calculated by Maxwell's equations [10], which mathematically describe the interdependence of the electromagnetic waves. The general form of Maxwell's equations is simplified to demonstrate the electromagnetic field of microwaves penetrated in the human body as the following equations:

$$\nabla \times \left(\frac{1}{\mu_r} \nabla \times E \right) - k_0^2 \left(\epsilon_r - \frac{j\sigma}{\omega\epsilon_0} \right) E = 0 \quad (1)$$

$$\epsilon_r = n^2 \quad (2)$$

where E is the electric field intensity (V/m), μ_r is the relative magnetic permeability, n is the refractive index, ϵ_r is the relative dielectric constant, $\epsilon_0 = 8.8542 \times 10^{-12}$ F/m is the permittivity of free space, and σ is the electric conductivity (S/m), $j = \sqrt{-1}$.

3.2.1 Boundary Condition for Wave Propagation Analysis. Microwave energy is emitted by a microwave high power device and strikes the human body with a particular power density. Therefore, boundary condition for electromagnetic wave, as shown in Fig. 3, is considered as follows.

It is assumed that the uniform wave flux strikes the left side of the human body. Therefore, at the left boundary of the considered domain, an electromagnetic simulator employs TE wave propagation port with a specified power density,

$$S = \int (E - E_1) \cdot E_1 / \int E_1 \cdot E_1 \quad (3)$$

Boundary conditions along the interfaces between different media, for example, between air and tissue or tissue and tissue, are considered as a continuity boundary condition,

$$n \times (H_1 - H_2) = 0 \quad (4)$$

The outer sides of the tissue boundaries are considered as a scattering boundary condition,

$$n \times (\nabla \times E_z) - jkE_z = -jk(1 - k \cdot n)E_{0z} \exp(-jk \cdot r) \quad (5)$$

3.3 Interaction of Electromagnetic Waves and Human Tissues. Interaction of electromagnetic fields with biological tissues can be defined in terms of SAR. Human tissues are generally lossy mediums for EM waves with finite electric conductivity. They are usually neither good dielectric materials nor good conductors.

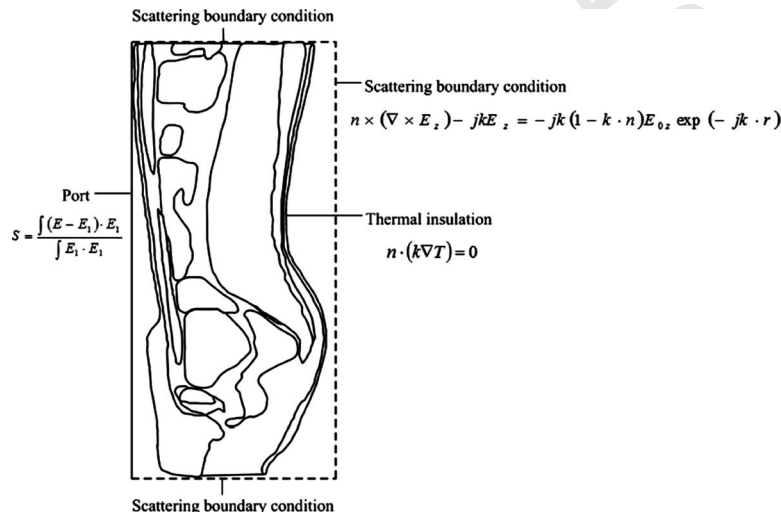


Fig. 3 Boundary condition for analysis

ductors. When EM waves propagate through the human tissues, the energy of EM waves is absorbed by the tissues. The specific absorption rate is defined as a power dissipation rate normalized by material density [8]. The specific absorption rate is given by

$$\text{SAR} = \frac{\sigma}{\rho} |E|^2 \quad (6)$$

where E is the root mean square electric field (V/m), σ is the conductivity (S/m), and ρ is the mass density of the tissue (kg/m^3).

3.4 Equations for Heat Transfer Analysis. The electric field within the model attenuates due to energy absorption. The absorbed energy is converted to thermal energy, which increases the tissue temperature. To solve the thermal problem, the temperature distribution in the human body has been evaluated by the coupled bioheat and Maxwell equations. The temperature distribution corresponded to the specific absorption rate. This is because the specific absorption rate within the human body distributes, owing to energy absorption. Thereafter, the absorbed energy is converted to thermal energy, which increases the tissue temperature.

Heat transfer analysis of the human body is modeled in two dimensions over the y-z plane. To simplify the problem, the following assumptions were made.

1. Human tissues are biomaterial with constant thermal properties.
2. No phase change in substance occurs within the tissues.
3. There is no energy exchange throughout the human body model.
4. There is no chemical reactions occur within the tissues.
5. Local thermodynamic equilibrium is considered.

Corresponding electromagnetic field and temperature profiles can also be assumed to be two dimensional in the y-z plane. There is a continuity boundary condition between the organs within the human body. The temperature distribution inside the human model is obtained by using Pennes' bioheat equation [19–23]. The transient bioheat equation effectively describes how transfer occurs within the human body, and the equation can be written as

$$\rho C \frac{\partial T}{\partial t} = \nabla \cdot (k \nabla T) + \rho_b C_b \omega_b (T_b - T) + Q_{\text{met}} + Q_{\text{ext}} \quad (7)$$

where ρ is the tissue density (kg/m^3), C is the heat capacity of tissue ($\text{J}/\text{kg K}$), k is the thermal conductivity of tissues ($\text{W}/\text{m K}$), T is the temperature ($^{\circ}\text{C}$), T_b is the temperature of blood ($^{\circ}\text{C}$), ρ_b is the density of blood before entering ablation region (kg/m^3), C_b is the specific heat capacity of blood ($\text{J}/\text{kg K}$), ω_b is the blood perfusion rate (1/s), Q_{met} is the metabolism heat source (W/m^3), and Q_{ext} is the external heat source (microwave heat-source density) (W/m^3).

In the analysis, heat conduction between tissues and blood flow is approximated by the term $\rho_b C_b \omega_b (T_b - T)$. The metabolism heat source is negligible, and therefore $Q_{\text{met}} = 0$.

The external heat source is equal to the resistive heat generated by electromagnetic field (microwave power absorbed), which defined as

$$Q_{\text{ext}} = \frac{1}{2} \sigma_{\text{tissue}} |\vec{E}|^2 \quad (8)$$

where $\sigma_{\text{tissue}} = 2\pi f G \epsilon_r' \epsilon_0$

3.4.1 Boundary Condition for Heat Transfer Analysis. The heat transfer analysis is considered only in the human body domain, which does not include parts of the surrounding space. As shown in Fig. 3, the boundaries of the human body are considered as an insulated boundary condition,

$$n \cdot (k \nabla T) = 0 \quad (9)$$

It is assumed that no contact resistance occurs between the internal organs of the human body. Therefore, the internal boundaries are assumed to be a continuity boundary condition,

$$n \cdot (k_u \nabla T_u - k_d \nabla T_d) = 0 \quad (10)$$

3.4.2 Initial Condition for Heat Transfer Analysis. For this analysis, the temperature distribution within the human body is assumed to be uniform. Therefore, the initial temperature of the human body is defined as

$$T(t_0) = 37^{\circ}\text{C} \quad (11)$$

The thermoregulation mechanisms and the metabolic heat generation of each tissue have been neglected to illustrate the clear temperature distribution. At the skin-air interface, the insulated boundary condition has been imposed to clearly illustrate the temperature distribution.

3.5 Calculation Procedure. To date, there are three principal techniques within computation electromagnetic (CEM): finite difference time domain method (FDTD) [2], method of moments (MOM) [10], and FEM. FEM has been extensively used in the simulation of electromagnetic field. Moreover, FEM models can provide users with quick and accurate solutions to multiple systems of differential equations.

In this research, the finite element method is used to analyze the transient problems. The computational scheme is to assemble finite element model and compute a local heat generation term by performing an electromagnetic calculation using tissue properties. In order to obtain a good approximation, a fine mesh is specified in the sensitive areas. This study provides a variable mesh method for solving the problem, as shown in Fig. 4. The coupled model of electromagnetic field and thermal field is solved by the FEM model, which was implemented using COMSOLTM MULTIPHYSICS 3.4, to demonstrate the phenomenon that occurs within the human body exposed to electromagnetic field. The study employs an implicit time step scheme to solve the electric field and temperature field. In this research, a time step of 10^{-2} s and 10^{-12} s are used to solve Maxwell's equations and bioheat equation, respectively. These are found to be practical to achieve each time step convergence. The temperature distribution has been evaluated by taking into account the specific absorption rate due to the electromagnetic field exposure at a particular frequency. Until the steady state is reached, the temperature at each time step is collected.

The 2D model is discretized using triangular elements, and the Lagrange quadratic is used to approximate temperature and SAR variation across each element. The convergence test of the frequency of 2450 MHz are carried out to identify the suitable number of elements required. The number of elements where solution is independent of mesh density is found to be 92,469. Higher numbers of elements are not tested due to lack of computational memory and performance. The convergence curve resulting from the convergence test is shown in Fig. 5.

4 Results and Discussion

In this study, the coupled mathematical model of bioheat transfer and electromagnetic wave propagation as well as the initial temperature of 37°C for all cases are used for the analysis. For the simulation, the thermal and dielectric properties are directly taken from Tables 1 and 2, respectively. The exposed leakage power density used in this study refers to the ICNIRP standard for safety level at the maximum SAR value of $10 \text{ W}/\text{kg}$ [3]. However, there are frequently exceeded values of leakage power density in the industrial working area due to the leakage of microwave from the microwave high power devices [3]. In the drying industry, only two microwave frequencies of 915 MHz and 2450 MHz are available. In this analysis, the effects of operating frequency (915 MHz and 2450 MHz) and leakage power density ($5 \text{ mW}/\text{cm}^2$, $10 \text{ mW}/\text{cm}^2$, $50 \text{ mW}/\text{cm}^2$, and $100 \text{ mW}/\text{cm}^2$) on distributions of specific absorption rate and temperature profile within the hu-

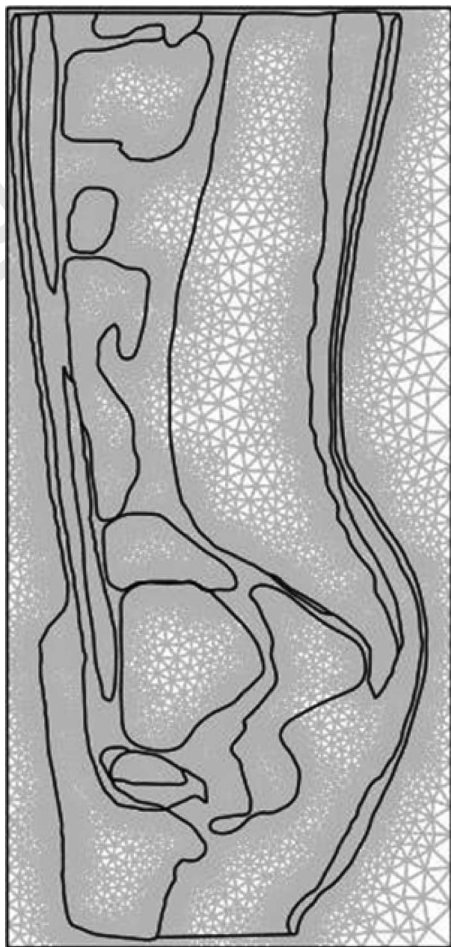


Fig. 4 An initial two-dimensional finite element mesh of human cross section model

man body are systematically investigated. The influences of frequencies and leakage power density on human body subject to electromagnetic wave are discussed in detail.

4.1 Verification of the Model. It must be noted in advance that it is not possible to make a direct comparison of the model in this study and the experimental results. In order to verify the accuracy of the present numerical model, the simple case of the simulated results is then validated against the numerical results

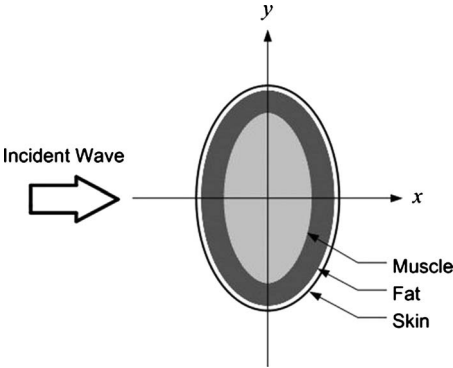


Fig. 6 Geometry of the validation model obtained from the paper [3]

with the same geometric model obtained by Nishizawa and Hashimoto [5]. The horizontal cross section of three-layer human tissues as shown in Fig. 6 is used in the validation case. In the validation case, the leakage power density exposed to the electromagnetic frequency of 1300 MHz is 1 mW/cm². The results of the selected test case are illustrated in Fig. 7 for SAR distribution in the human body. Table 3 clearly shows a good agreement in the maximum value of the SAR of tissues between the present solution and that of Nishizawa and Hashimoto. This favorable comparison lends confidence in the accuracy of the present numerical model. It is important to note that there may be some errors occurring in the simulations, which are generated by the input dielectric properties and the numerical scheme.

4.2 Distribution of Electric Field. To illustrate the distribution of penetrated electric field inside each organ of the human body, simulation analysis is required. Figure 8 shows the simulation of electric field pattern inside the human body exposed to electromagnetic field of TE mode propagation along the vertical cross section human body model at the frequencies of 915 MHz and 2450 MHz.

Figure 8(a) shows the distribution of electric field at the frequency of 915 MHz. It is found that a large part of electromagnetic wave at 915 MHz can penetrate further into the body. This electric field leads to deeper electromagnetic energy absorbed in the organs of human body in comparison to the frequency of 2450 MHz, which will be discussed later. With the lower frequency, a large part of electromagnetic wave is able to penetrate into the human body due to its long wavelength, which corresponds to a larger penetration depth.

Figure 8(b) shows the distribution of electric field at the frequency of 2450 MHz.

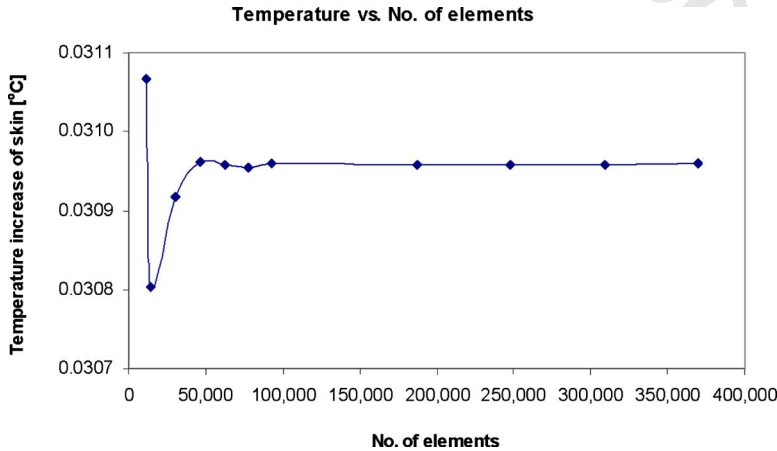


Fig. 5 Grid convergence curve of the 2D model

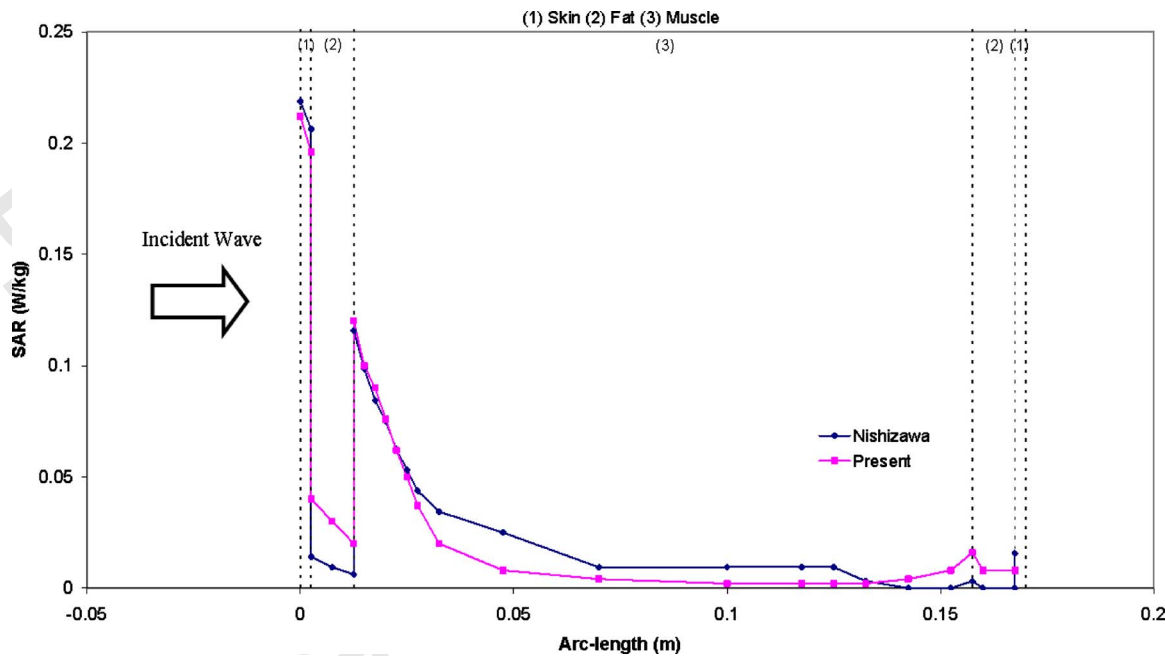


Fig. 7 Comparison of the calculated SAR distribution to the SAR distribution obtained by Nishizawa and Hashimoto [5]

quency of 2450 MHz. A high frequency wave has a short wavelength that corresponds to a small penetration depth of the electromagnetic wave. It is found that the electric field diminishes within very small distances, which results in a low specific absorption rate in organs deep inside the human trunk. This phenomenon explains why the electric field and therefore the specific absorption rate are greatest at the skin and decay sharply along the propagation direction for a short wavelength. It can be seen that the distribution of electric field for the higher frequency occurs in

the outer parts of the body, especially in skin, fat, and muscle. The maximum electric field intensities are 91.51 V/m at the frequency of 915 MHz and 56.12 V/m at the frequency of 2450 MHz. The electric field within the human body is extinguished where the electric field attenuates due to absorbed electromagnetic energy and is converted to heat.

4.3 SAR Distribution in Human Tissues. Figure 9 shows the SAR distribution evaluated on the vertical section of the human body in which the maximum SAR value occurs. It is evident from the results that the dielectric properties, as shown in Table 1, can become significant on SAR distribution in human tissues when microwave energy is exposed in these tissues. The magnitude of dielectric properties in each organ will directly affect the amount of SAR within the human body. The highest SAR values are obtained in the region of the skin for the frequency of 915 MHz at 3.43 W/kg and for the frequency of 2450 MHz at 3.02 W/kg. It is found that the SAR distribution in the human model is

Table 3 Comparison of the results obtained in the present study with those of Nishizawa and Hashimoto [5]

	Present work	Published work [5]	% Difference
SAR _{max} in skin	0.212	0.220	3.63
SAR _{max} in fat	0.198	0.206	3.88
SAR _{max} in muscle	0.116	0.120	3.33

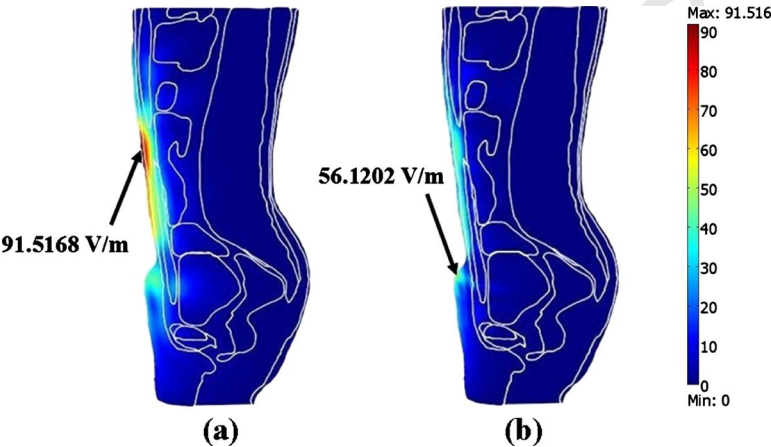


Fig. 8 Electric field distribution in human body (V/m) exposed to the leakage power density of 5 mW/cm² at the frequencies of (a) 915 MHz and (b) 2450 MHz

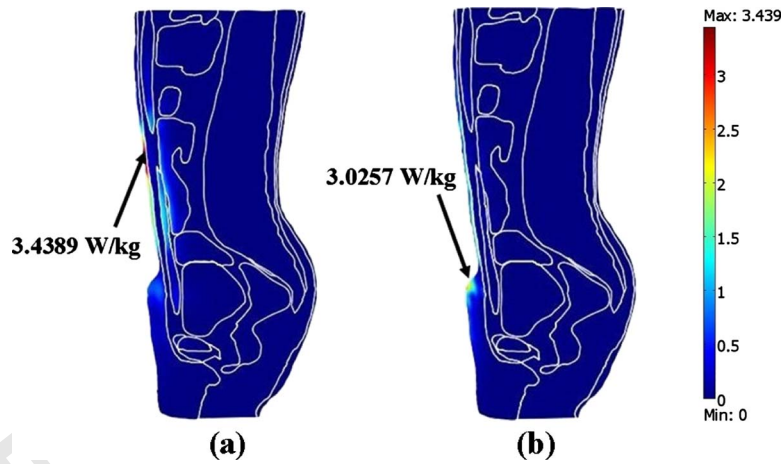


Fig. 9 SAR distribution in human body (W/kg) exposed to the leakage power density of 5 mW/cm² at the frequencies of (a) 915 MHz and (b) 2450 MHz

different due to the effect of the frequency and the dielectric properties of human tissues. From Fig. 9, it appears that for the frequency of 915 MHz, the highest SAR values also occur in the muscle and the small intestine due to the effect of high values of the dielectric properties. Comparing to the ICNIRP limit of SAR values (2 W/kg), the resulting SAR values are exceeded in all cases.

4.4 Temperature Distribution. Figure 10 shows the temperature increase of the organs in human body exposed to electromagnetic waves at various times. For the human body exposed to the leakage of electromagnetic wave from a high power microwave heating device at the frequency of 915 MHz or 2450 MHz for a period of time, the temperature within the human body (Fig. 13) is increased corresponding to the specific absorption rate (Fig. 12). This is because the electric field within the human body attenuates, owing to the energy absorbed, and thereafter the absorbed energy is converted to thermal energy, which increases the human body temperature. It is found that at the different frequencies, the distribution patterns of temperature at a particular time are quite different. The hot spot zone is strongly displayed at the 10 min for the frequency of 915 MHz, owing to the extensive penetration depth and different properties of tissues. To a lesser extent, at the frequency of 2450 MHz, the temperature increases in the human body are always found at the periphery of the body correlated with the electric field and SAR (Figs. 8 and 9). For the case of microwave frequency at 915 MHz, the highest temperature of 37.0487°C occurs in the fat, as shown in Fig. 10(a). A different pattern of temperature distribution is obtained at the 2450 MHz frequency, as shown in Fig. 10(b), in which the highest temperature of 37.0311°C is presented in the skin. The maximum temperature increases, with the leakage power density of 5 mW/cm², at the 915 MHz and 2450 MHz frequencies are 0.048°C and 0.031°C, respectively. These are much lower than the thermal damage temperature within the range of 1–5°C.

An electromagnetic wave exposure (for example, the leakage from microwave heating system) usually lasts only a few minutes; hence, the steady-state temperature rise is rarely reached, except for workers who work in the leakage area. Figures 11 and 12 show the temperature distributions inside the human body at the 915 MHz and 2450 MHz frequencies for different exposure times. At 915 MHz, fat tissue temperature increases slower than the other tissues due to its low lossy behavior. Fat tissue also has maximum steady-state temperature due to its low blood perfusion rate. It is found that at 915 MHz, the internal tissues (fat and bone) reach steady state slower than the external tissues (skin) due to the low thermal conductivity of the fat tissue. However, at 2450 MHz, all

of the temperature increases can reach steady state within a short period due to the high thermal conductivity of the skin tissue as well as the low heat capacity of the fat tissue.

4.5 Comparison of SAR Distribution and Temperature Distribution in Human Tissues. Consider the relation of SAR and temperature distribution at the extrusion line (Fig. 13), temperature increases of human tissues are induced by local dissipation of SAR. For a human exposed to the leakage power density of 5 mW/cm², Fig. 14 shows the maximum SAR of the 2450 MHz frequency (2.0 W/kg) in the skin region. The maximum SAR value of the 2450 MHz is approximately equal to the maximum SAR value of the 915 MHz frequency (2.0 W/kg) in the skin. However, Fig. 15 shows that the maximum temperature increase of the 2450 MHz frequency in the skin (0.02°C) is lower than the maximum temperature increase of the 915 MHz frequency in the fat (0.03°C). These different behaviors are due to the fact that for the same SAR value at different frequencies, the temperature increase is different. The maximum SAR of the 2450 MHz frequency induces the temperature increase in the skin that is lower than the temperature increase in the fat of the 915 MHz frequency. Consequently, since the interior of the fat region has a lower blood perfusion rate (4.58×10^{-4} 1/s) than the skin (0.02 1/s) and fat is bounded by low thermal conductivity tissue (skin), the heat transfer of fat from blood perfusion is less effective. At the same time, the high blood perfusion is present in the skin.

The localized maximum SAR for the frequencies of 915 MHz and 2450 MHz is shown in Fig. 16. For the value of localized SAR for each organ, it is found that SAR increases as the frequency decreases. For both frequencies, the three highest SARs are shown for skin, muscle, and small intestine. Furthermore, the localized SARs of the 915 MHz frequency are higher than the 2450 MHz frequency in all organs.

The maximum localized temperature increases in all tissues for the frequency of 915 MHz and 2450 MHz are shown in Fig. 17. The maximum temperature increase occurs in fat at the 915 MHz frequency, whereas the maximum temperature increase appears in the skin tissues at the 2450 MHz frequency. Since the penetration depth of the 915 MHz microwave frequency is larger than the 2450 MHz frequency and the inner organs have high dielectric properties, the larger temperature increases of the 915 MHz frequency are particularly high in the inner tissues (small intestine and bladder).

As a result, the human heterogeneous tissues greatly influence the temperature increases in the skin region exposed to the frequency of 2450 MHz and in the fat region for the frequency of

AQ: #3

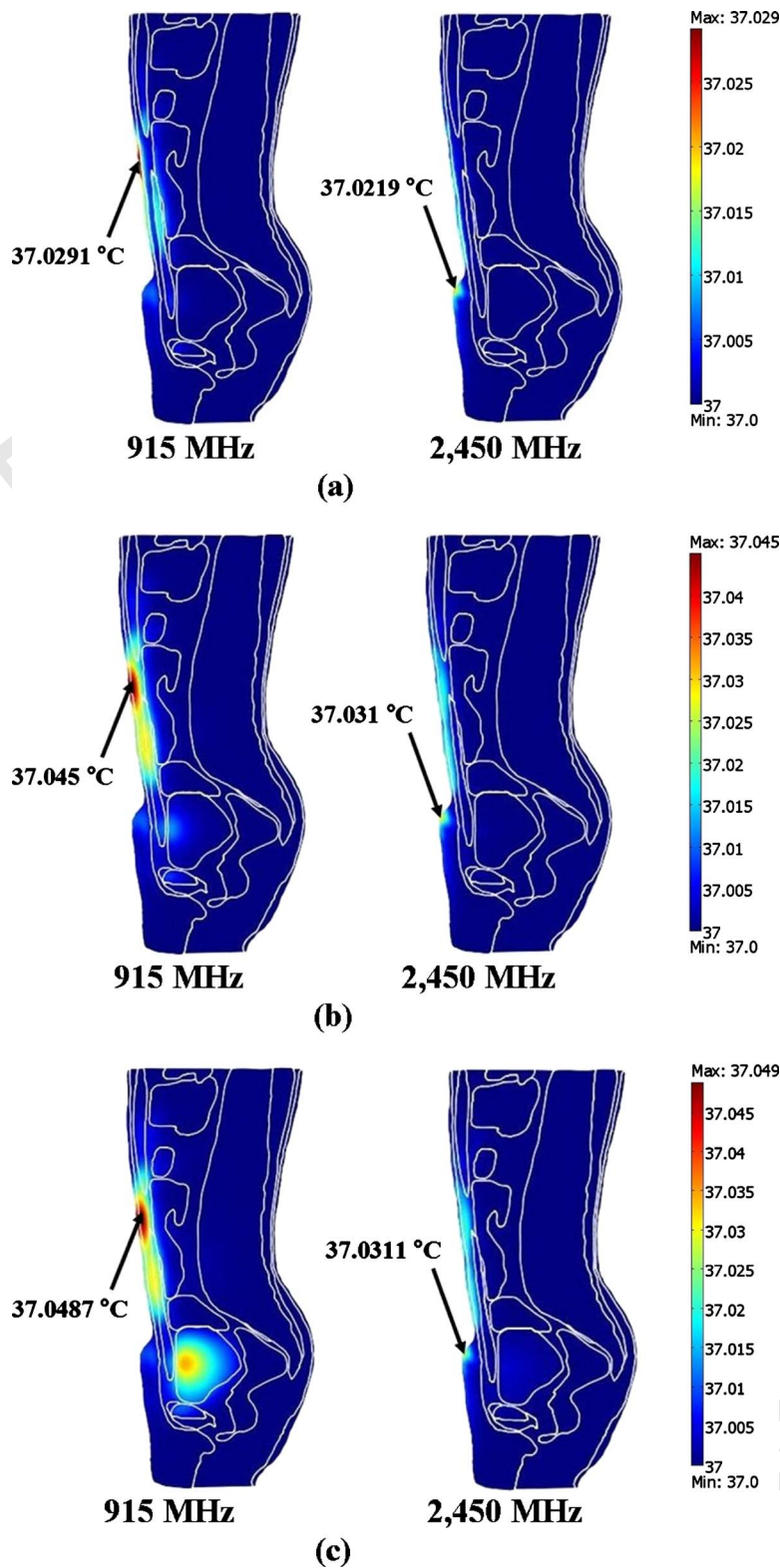


Fig. 10 The temperature distribution of human body exposed to electromagnetic wave at the frequencies of 915 MHz and 2450 MHz: (a) 1 min, (b) 10 min, and (c) steady state

915 MHz. It is found that the temperature distributions are not proportional to the local SAR values. Nevertheless, these are also related to the parameters such as thermal conductivity, dielectric properties, and blood perfusion rate. It is therefore important to

use a thermal model couple with electromagnetic wave propagation model to assess the health risk in terms of temperature increase from electromagnetic exposure.

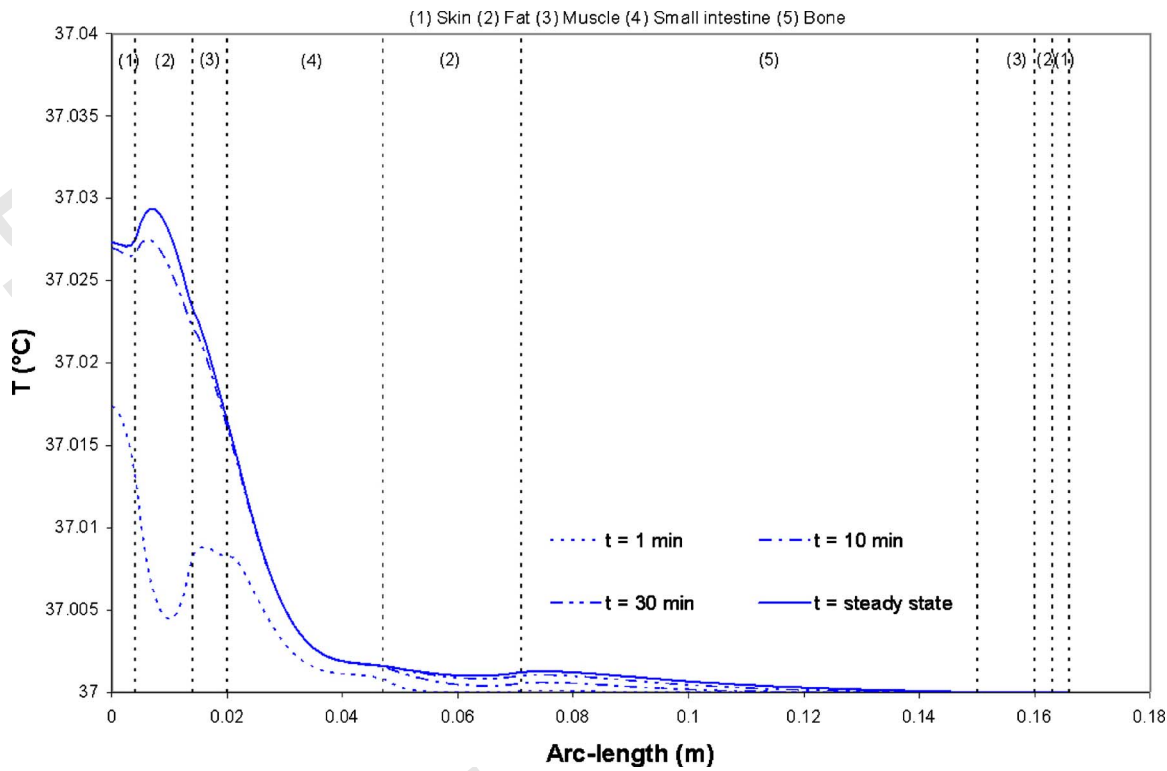


Fig. 11 Temperature distribution versus arc length of human body at various times exposed to the electromagnetic frequency of 915 MHz at the leakage power density of 5 mW/cm²

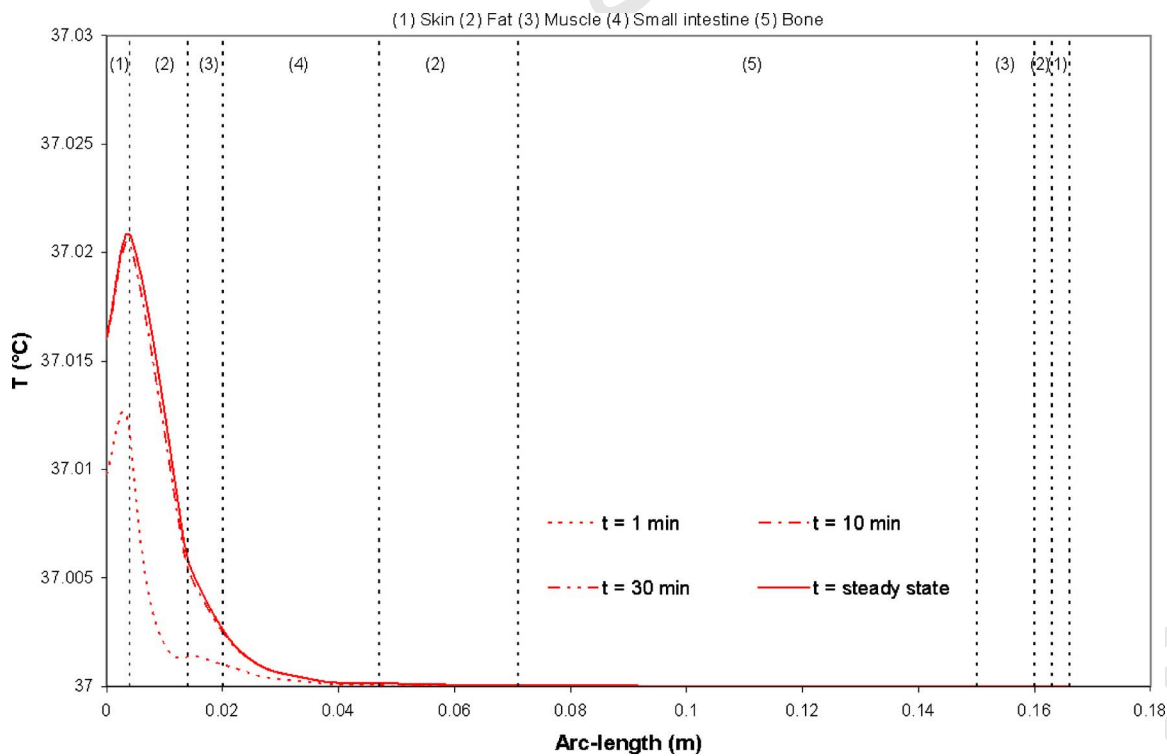


Fig. 12 Temperature distribution versus arc length of human body at various times exposed to the electromagnetic frequency of 2450 MHz at the leakage power density of 5 mW/cm²

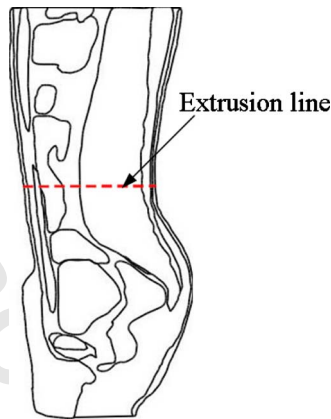


Fig. 13 The extrusion line in the human body where the SAR and temperature distribution are considered

4.6 Effect of Leakage Power Density. The effect of leakage power density (the power irradiated on the human surface) has also been investigated. The incident power and leakage power density are related, as shown in Table 4. Figure 18 shows the comparison of the temperature increase distribution within the human body at various incident powers, at $t=1$ min, with the frequency of 915 MHz, along the extrusion line (Fig. 11). Figure 19 shows the temperature fields of human body exposed to the electromagnetic frequency of 915 MHz at $t=1$ min corresponding to leakage power densities, as shown in Table 4. It is found that incident power significantly influences the rate of temperature increase. Greater power provides greater heat generation inside the human body, thereby increasing the rate of temperature rise.

5 Conclusions

This study presents the numerical simulation SAR and temperature distribution in the human body exposed to electromagnetic field at the frequencies of 915 MHz and 2450 MHz with the power densities of 5 mW/cm², 10 mW/cm², 50 mW/cm², and 100 mW/cm². The numerical simulations in this study show several important features of the energy absorption in the human body. The results show that the maximum temperatures in various organs are significantly different at different frequencies. The maximum temperature is found at the skin for the frequency of 2450 MHz and is found at the fat for the frequency of 915 MHz. While the maximum SAR value in both frequencies are found at the skin. It is found that greater leakage power density results in a greater heat generation inside the human body, thereby increasing the rate of temperature increase. Moreover, it is found that the temperature distributions in human body induced by electromagnetic fields are not directly related to the SAR distribution due to the effect of dielectric properties, thermal properties, blood perfusion, and penetration depth of the microwave power.

Therefore, health effect assessment of electromagnetic wave at various frequencies requires the utilization of the numerical simulation of SAR model along with the thermal model. However, the dielectric properties of some tissues are not indicated as a function of frequency due to the limited number of human tissue dielectric properties in the literature, and this may affect the accuracy of the simulation results. Future works will focus on the frequency-dependent dielectric properties of human tissue. A study will also be developed for 3D simulations and the study of the temperature dependency of dielectric properties. This will allow a better understanding of the realistic situation of the interaction between the electromagnetic field and the human tissues.

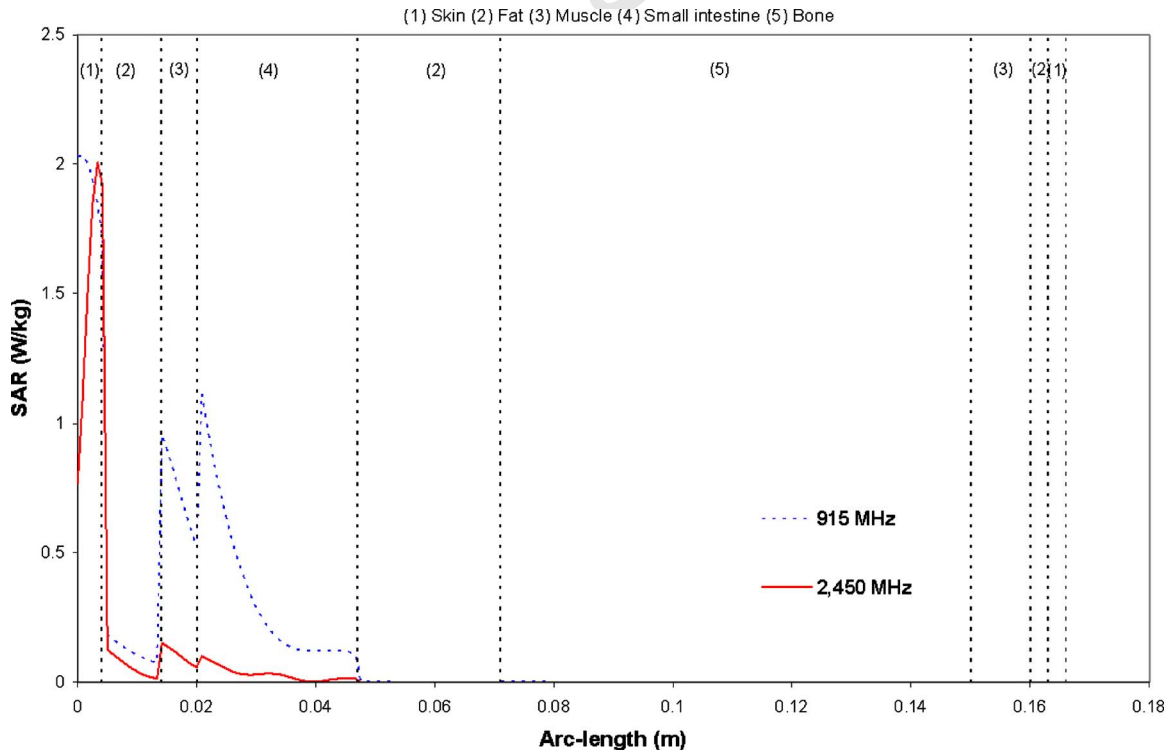


Fig. 14 SAR distribution versus arc length of human body exposed to the leakage power density of electromagnetic field at the 5 mW/cm²

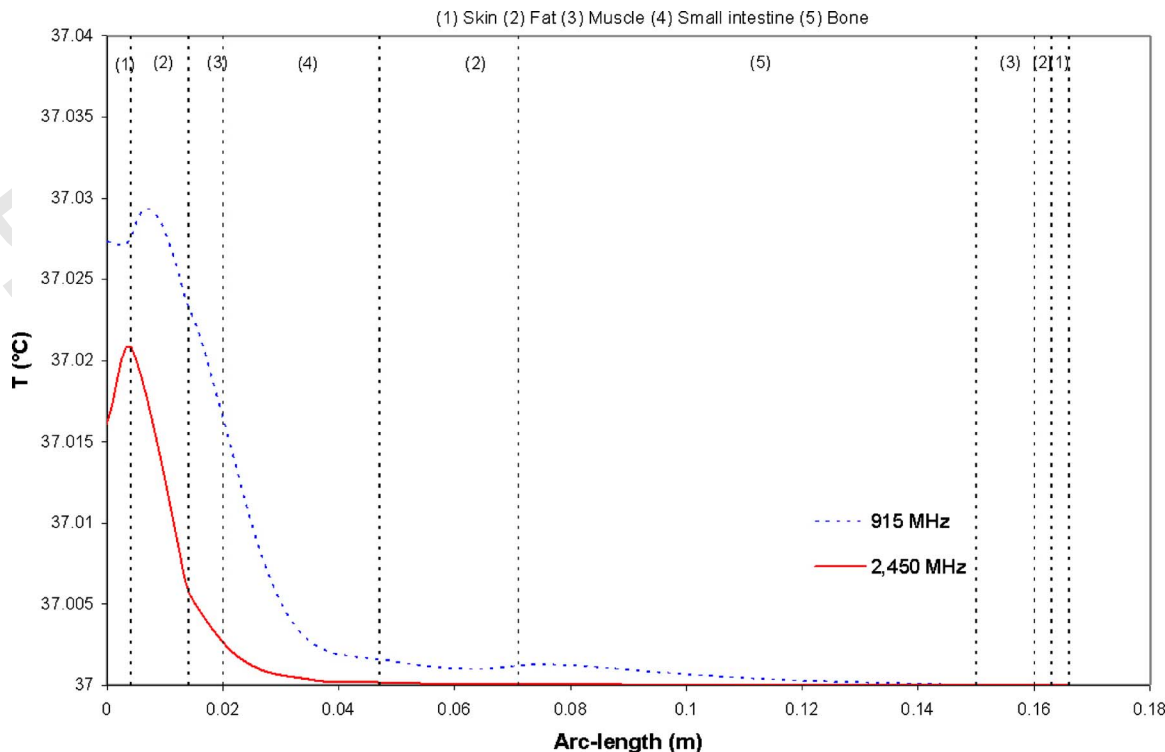


Fig. 15 Temperature distribution versus arc length of the human body exposed to the leakage power density of electromagnetic field at 5 mW/cm²

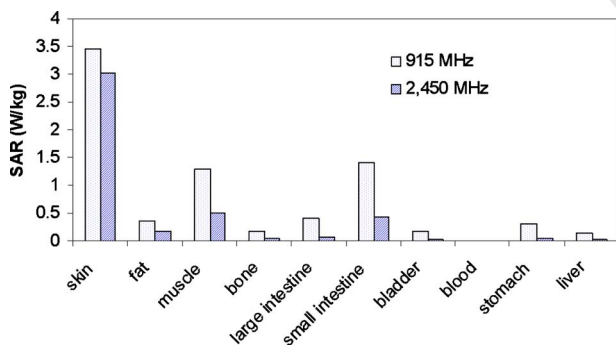


Fig. 16 Comparison of the maximum SAR in human tissues at the frequencies of 915 MHz and 2450 MHz

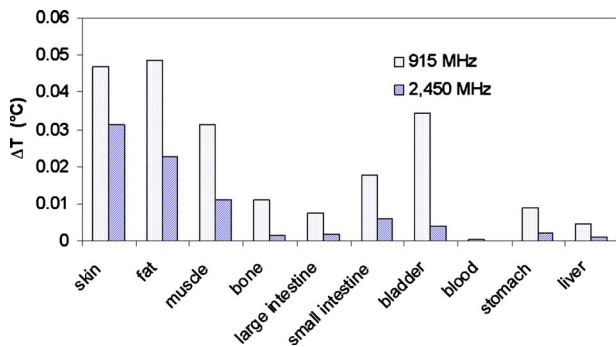


Fig. 17 Comparison of the temperature increases in human tissues at the frequencies of 915 MHz and 2450 MHz

Table 4 The relationship between the incident power and the leakage power density of microwave

Incident power (W)	Power density (mW/cm ²)
10.5	5
21.0	10
105	50
210	100

Acknowledgment

The authors would like to express their appreciation to the Thailand Research Fund (TRF) and the Thai Commission on Higher Education (CHE) for providing financial support for this study.

Nomenclature

- C = specific heat capacity (J/(kg K))
- E = electric field intensity (V/m)
- f = frequency of incident wave (Hz)
- j = current density
- k = thermal conductivity (W/(m K))
- n = refractive index
- Q = heat source (W/m³)
- T = temperature (K)
- t = time
- $\tan \delta$ = loss tangent coefficient

Greek Letters

- μ = magnetic permeability (H/m)
- ϵ = permittivity (F/m)
- σ = electric conductivity (S/m)
- ω = angular frequency (rad/s)

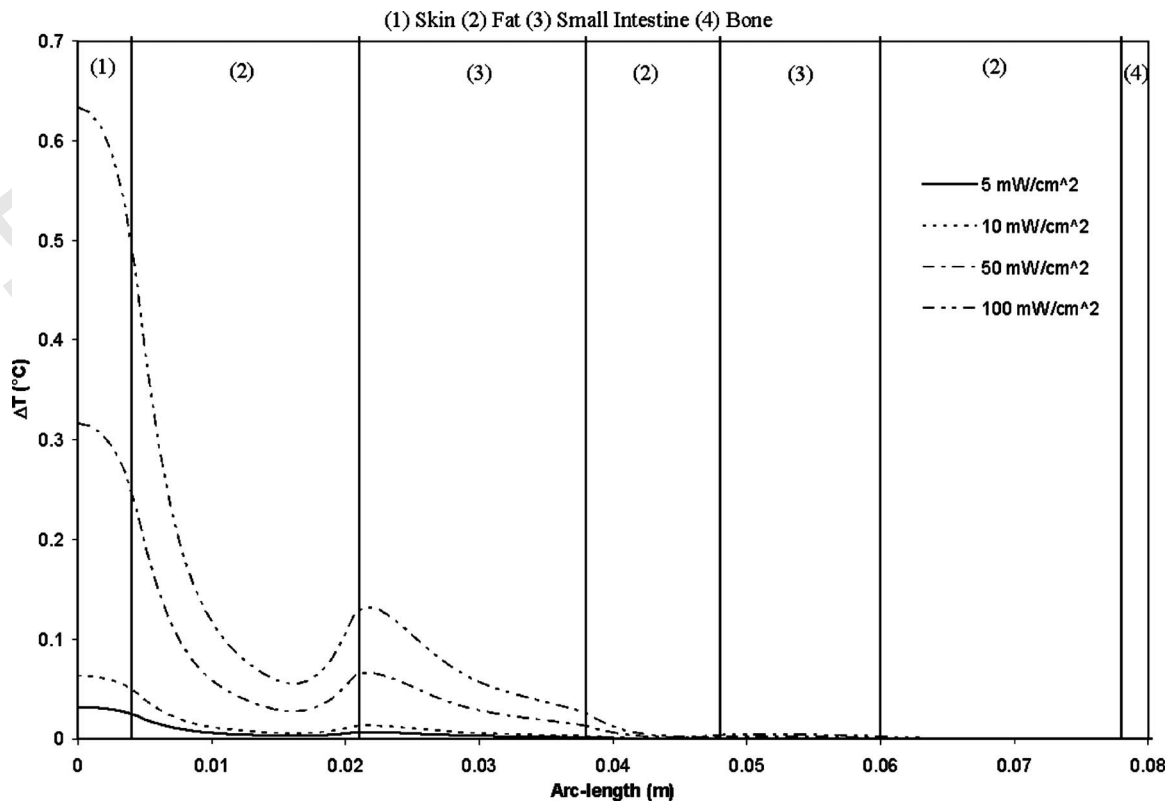


Fig. 18 Temperature increase versus arc length of human body exposed to the electromagnetic frequency of 915 MHz at various leakage power densities, at $t=1$ min

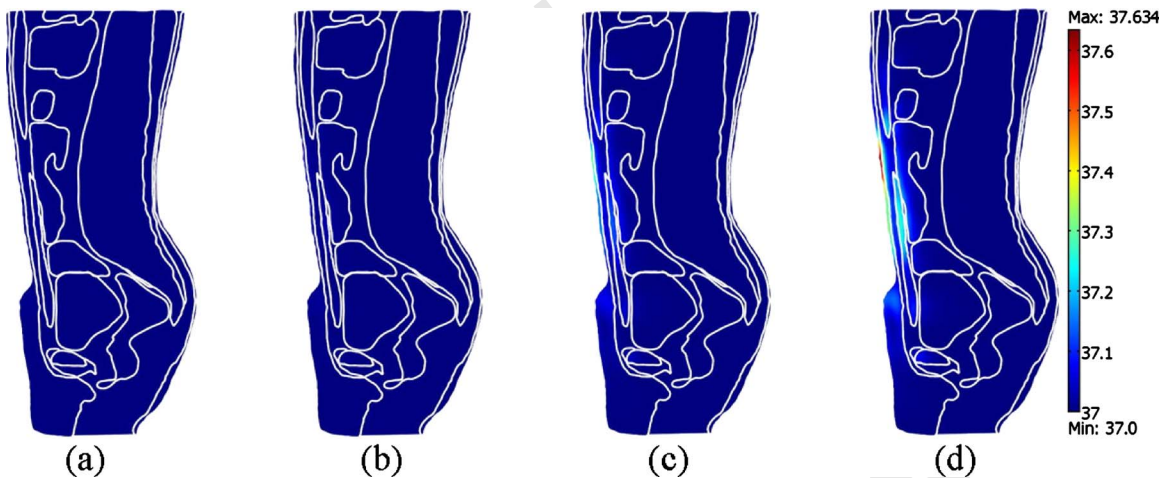


Fig. 19 Temperature distribution of human body exposed to the electromagnetic frequency of 915 MHz at $t=1$ min at various leakage power densities: (a) 5 mW/cm², (b) 10 mW/cm², (c) 50 mW/cm², and (d) 100 mW/cm²

ρ = density (kg/m³)
 ω_b = blood perfusion rate (1/s)

Subscripts
 b = blood
 ext = external
 met = metabolic
 r = relative
 0 = free space, initial condition

References

[1] Rattanadecho, P., Suwannapum, N., and Cha-um, W., 2009, "Interactions Be-

tween Electromagnetic and Thermal Fields in Microwave Heating of Hardened Type I-Cement Paste Using a Rectangular Waveguide (Influence of Frequency and Sample Size)," ASME J. Heat Transfer, **131**, p. 082101.
[2] Ratanadecho, P., Aoki, K., and Akahori, M., 2002, "Influence of Irradiation Time, Particle Sizes, and Initial Moisture Content During Microwave Drying of Multi-Layered Capillary Porous Materials," ASME J. Heat Transfer, **124**, pp. 151–161.
[3] Ziegelberger, G., 2009, "ICNIRP Statement on the 'Guidelines for Limiting Exposure to Time-Varying Electric, Magnetic, and Electromagnetic Fields (up to 300 GHz)'," Health Phys., **97**(3), pp. 257–258.
[4] Stuchly, M. A., 1995, "Health Effects of Exposure to Electromagnetic Fields," IEEE Aerospace Applications Conference Proceedings, pp. 351–368.
[5] Nishizawa, S., and Hashimoto, O., 1999, "Effectiveness Analysis of Lossy Dielectric Shields for a Three-Layered Human Model," IEEE Trans. Microwave Theory Tech., **47**(3), pp. 277–283.

[6] Seufi, A. M., Ibrahim, S. S., Elmaghraby, T. K., and Hafez, E. E., 2009, "Preventive Effect of the Flavonoid, Quercetin, on Hepatic Cancer in Rats via Oxidant/Antioxidant Activity: Molecular and Histological Evidences," *J. Exp. Clin. Cancer Res.*, **28**(1), p. 80.

[7] Yang, D., Converse, M. C., Mahvi, D. M., and Webster, J. G., 2007, "Measurement and Analysis of Tissue Temperature During Microwave Liver Ablation," *IEEE Trans. Biomed. Eng.*, **54**(1), pp. 150–155.

[8] Kanai, H., Marushima, H., Kimura, N., Iwaki, T., Saito, M., Maehashi, H., Shimizu, K., Muto, M., Masaki, T., Ohkawa, K., Yokoyama, K., Nakayama, M., Harada, T., Hano, H., Hataba, Y., Fukuda, T., Nakamura, M., Totsuka, N., Ishikawa, S., Unemura, Y., Ishii, Y., Yanaga, K., and Matsuura, T., 2007, "Extracorporeal Bioartificial Liver Using the Radial-Flow Bioreactor in Treatment of Fatal Experimental Hepatic Encephalopathy," *Artif. Organs*, **31**(2), pp. 148–151.

[9] Pennes, H. H., 1998, "Analysis of Tissue and Arterial Blood Temperatures in the Resting Human Forearm," *J. Appl. Physiol.*, **85**(1), pp. 5–34.

[10] Spiegel, R. J., 1984, "A Review of Numerical Models for Predicting the Energy Deposition and Resultant Thermal Response of Humans Exposed to Electromagnetic Fields," *IEEE Trans. Microwave Theory Tech.*, **32**(8), pp. 730–746.

[11] Dragun, V. L., Danilova-Tret'yak, S. M., and Gubarev, S. A., 2005, "Simulation of Heating of Biological Tissues in the Process of Ultrahigh-Frequency Therapy," *J. Eng. Phys. Thermophys.*, **78**(1), pp. 109–114.

[12] Ozen, S., Helhel, S., and Cerezci, O., 2008, "Heat Analysis of Biological Tissue Exposed to Microwave by Using Thermal Wave Model of Bio-Heat Transfer (TWMBT)," *Burns*, **34**(1), pp. 45–49.

[13] Samaras, T., Christ, A., Klingenbock, A., and Kuster, N., 2007, "Worst Case Temperature Rise in a One-Dimensional Tissue Model Exposed to Radiofrequency Radiation," *IEEE Trans. Biomed. Eng.*, **54**(3), pp. 492–496.

[14] Wang, J., and Fujiwara, O., 1999, "FDTD Computation of Temperature Rise in the Human Head for Portable Telephones," *IEEE Trans. Microwave Theory Tech.*, **47**(8), pp. 1528–1534.

[15] Hirata, A., Morita, M., and Shiozawa, T., 2003, "Temperature Increase in the Human Head Due to a Dipole Antenna at Microwave Frequencies," *IEEE Trans. Electromagn. Compat.*, **45**(1), pp. 109–116.

[16] Hirata, A., Wang, J., Fujiwara, O., Fujimoto, M., and Shiozawa, T., 2005, "Maximum Temperature Increases in the Head and Brain for SAR Averaging Schemes Prescribed in Safety Guidelines," *IEEE International Symposium on Electromagnetic Compatibility*, Chicago, IL, Vol. 3, pp. 801–804.

[17] Garcia-Fernandez, M. A., Valdes, J. F. V., Martinez-Gonzalez, A. M., and Sanchez-Hernandez, D., 2007, "Electromagnetic Heating of a Human Head Model by a Half-Wavelength Dipole Antenna," *The Second European Conference on Antennas and Propagation*, pp. 1–4.

[18] Shiba, K., and Higaki, N., 2009, "Analysis of SAR and Current Density in Human Tissue Surrounding an Energy Transmitting Coil for a Wireless Capsule Endoscope," *2009 20th International Zurich Symposium on Electromagnetic Compatibility*, Zurich, pp. 321–324.

[19] Yang, D., Converse, M. C., Mahvi, D. M., and Webster, J. G., 2007, "Expanding the Bioheat Equation to Include Tissue Internal Water Evaporation During Heating," *IEEE Trans. Biomed. Eng.*, **54**(8), pp. 1382–1388.

[20] Saito, K., Hiroe, A., Kikuchi, S., Takahashi, M., and Ito, K., 2006, "Estimation of Heating Performances of a Coaxial-Slot Antenna With Endoscope for Treatment of Bile Duct Carcinoma," *IEEE Trans. Microwave Theory Tech.*, **54**(8), pp. 3443–3449.

[21] Lang, J., Erdmann, B., and Seebass, M., 1999, "Impact of Nonlinear Heat Transfer on Temperature Control in Regional Hyperthermia," *IEEE Trans. Biomed. Eng.*, **46**(9), pp. 1129–1138.

[22] See, T. S. P., and Zhi, N. C., 2005, "Effects of Human Body on Performance of Wearable PIFAs and RF Transmission," *Antennas and Propagation Society International Symposium*, 2005 IEEE, Washington, DC, Vol. 1B, pp. 686–689.

[23] Chang, I., 2003, "Finite Element Analysis of Hepatic Radiofrequency Ablation Probes Using Temperature-Dependent Electrical Conductivity," *Biomed. Eng. Online*, **2**(12), pp. 1–18.

AUTHOR QUERIES — 005104JHR

- #1

Au: Please verify if “EM” means “electromagnetic.”
- #2

Au: Please check our insertion of Refs. 20–23
- #3

Au: Please check our insertion of “equal.”
- here.